CHAPTER 3

HYDROGENATION OF *CIS*-1,4-POLYISOPRENE CATALYZED BY $Ru(CH=CH(Ph))Cl(CO)(PCy_3)_2$

Polyisoprene is a diene polymer, which is a polymer made from the isoprene monomer, which contains two carbon - carbon double bonds. Like most diene polymers, it has carbon - carbon double bonds in its backbone chain. $Ru(CH=CH(Ph))Cl(CO)(PCy_3)_2$ has been reported to be an active catalyst for the selective hydrogenation of carbon - carbon double bonds in acrylonitrile-butadiene copolymers (Martin et al., 1997). In order to investigate the hydrogenation of polyisoprene in the presence of $Ru(CH=CH(Ph))Cl(CO)(PCy_3)_2$ in detail, comprehensive kinetic studies for this system were undertaken. It was hoped that the kinetic information combined with the spectroscopic experiments might offer sufficient clues to further the study of natural rubber hydrogenation.

A major objective of this thesis is to investigate the efficiency of the reaction involved in the quantitative hydrogenation of CPIP as well as to gain insight into the nature of the hydrogenation mechanism. The effect of catalyst level, concentration of polymer, hydrogen pressure and temperature were studied. In this chapter, the kinetics and mechanism for CPIP hydrogenation by $Ru(CH=CH(Ph))Cl(CO)(PCy_3)_2$ are presented and discussed.

3.1 FTIR and NMR Spectroscopic Characterization

The FTIR spectra of CPIP and the completely hydrogenated *cis*-1,4-polyisoprene (HCPIP) are shown in Figure 3.1. On comparing the spectrum of CPIP with that of HCPIP, it can be seen that the bands at 1664 and 837 cm^{-1} due to C=C stretching and olefinic C-H bending disappear, suggesting quantitative hydrogenation of CPIP. A peak appears at 735 cm^{-1} due to the presence of $-(CH_2)_3-$ groups during the hydrogenation process.

The final degree of hydrogenation of hydrogenated polymer was determined by ^{1}H-NMR. A typical ^{1}H-NMR spectrum of CPIP (a) together with the spectrum of the hydrogenated CPIP product (b) is shown in Figure 3.2. The hydrogenation led to the reduction in the peaks of isoprene units at 1.7, 2.2 and 5.2 ppm which are assigned to $-CH_3$, $-CH_2-$, and =CH groups, respectively and the emergence of new peaks at 0.8

and 1.1 – 1.8 ppm, attributed to the propylene-ethylene block of the hydrogenated product.

^{13}C-NMR spectrum of hydrogenated CPIP confirms that the polymer product is a strictly an alternating copolymer of ethylene-propylene (Figure 3.3). The peak areas at 138.2 and 122.8 ppm, which are indicative of olefinic carbon, disappear completely and four new peaks appear at 37.8, 33.1, 24.8 and 20.0 ppm, which are attributed to C_α, -CH-, C_β, and $-CH_3$ carbons, respectively. This confirms a quantitative hydrogenation of the carbon - carbon unsaturation.

3.2 Hydrogenation Catalyzed by Various Ru(II) Complexes

A number of ruthenium(II) bulky phosphine complexes were studied to gain insight into the effect of ligand choice on the activity and selectivity of the catalyst. All runs were carried out at the base set of conditions at 160°C, P_{H2} = 40.3 bar, [C=C] = 260 mM in 150 mL solution.

The results for the catalytic hydrogenation of CPIP using various Ru(II) complexes are summarized in Table 3.1. It is seen that Ru(CH=CH(Ph))Cl(CO)$(PCy_3)_2$, Ru(CH=CH(Ph))Cl(CO)$(PPr^i_3)_2$, RuCl(CO)H$(PPh_3)_3$ and RuCl(CO)$(PhCO_2)$ $(PPh_3)_2$ had similar activity (86 - 93% olefin conversion after 5 hours) with respect to the catalytic hydrogenation of CPIP. One of the easiest ruthenium complexes to prepare is $RuCl_2(PPh_3)_3$, which has been found to be an efficient catalyst for hydrogenation of polybutadiene under mild condition (Rao et al., 2001). However, for *cis*-1,4-polyisoprene, $RuCl_2(PPh_3)_3$ was not efficient for the hydrogenation (only 25% olefin conversion was attained after 5 hours of reaction). The hydrogenation of CPIP using π-$C_3H_5Ru(CO)_3Cl$ as catalyst was examined; however, it was only possible to achieve 48% hydrogenation after 5 hours of reaction and furthermore this catalyst system led to degradation of the polymer chain and isomerization. 1,2-Polyisoprene was also produced during the reduction process; its IR spectrum shows a characteristic peak at 968 cm^{-1}. Recently, $RuCl_2(CHC_6H_5)(PCy_3)_2$ has been found to be an olefin metathesis catalyst with high activity and stability (Trnka et al., 2001). Unlike for the case of olefin metathesis, the hydrogenation of CPIP with $RuCl_2$ $(CHC_6H_5)(PCy_3)_2$ was found to be less effective, only 63% hydrogenation could be achieved after 5 hours.

Based on these initial experimental results, Ru(CH=CH(Ph))Cl(CO)$(PCy_3)_2$ was chosen as the preferred Ru catalyst for a kinetic investigation of CPIP hydrogenation

in chlorobenzene as it exhibited the highest activity among the Ru complexes screened in this investigation. Furthermore, this styryl catalyst was remarkable air-stable.

Table 3.1: The Results of Hydrogenation of CPIP Using Ru(II) Complexes.

Catalyst	[Catalyst] (μM)	Co-catalyst	Solvent	% Hydrogenation
$Ru(CH=CH(Ph))Cl(CO)(PCy_3)_2$	80	none	Toluene	90.1
$Ru(CH=CH(Ph))Cl(CO)(PPr^i_3)_2$	80	none	Toluene	85.6
$RuCl(CO)H(PPh_3)_3$	80	none	Toluene	87.6
$RuCl(CO)(PhCO_2)(PPh_3)_2$	80	none	Toluene	89.0
$Ru(CH=CH(Ph))Cl(CO)(PCy_3)_2$	80	none	MCB	93.0
$Ru(CH=CH(Ph))Cl(CO)(PPr^i_3)_2$	80	none	MCB	90.2
$RuCl_2(PPh_3)_3$	80	PPh_3	MCB	24.8
π-$C_3H_5Ru(CO)_3Cl$	240	none	MCB	48.0
$RuCl_2(CHC_6H_5)(PCy_3)_2$	80	none	MCB	62.7

Conditions: T = 160°C; P_{H2} = 40.3 bar; [C=C] = 260 mM; reaction time = 5 h.
[C=C] is defined as the weight of *cis*-1,4-polyisoprene divided by molecular weight of repeating unit.

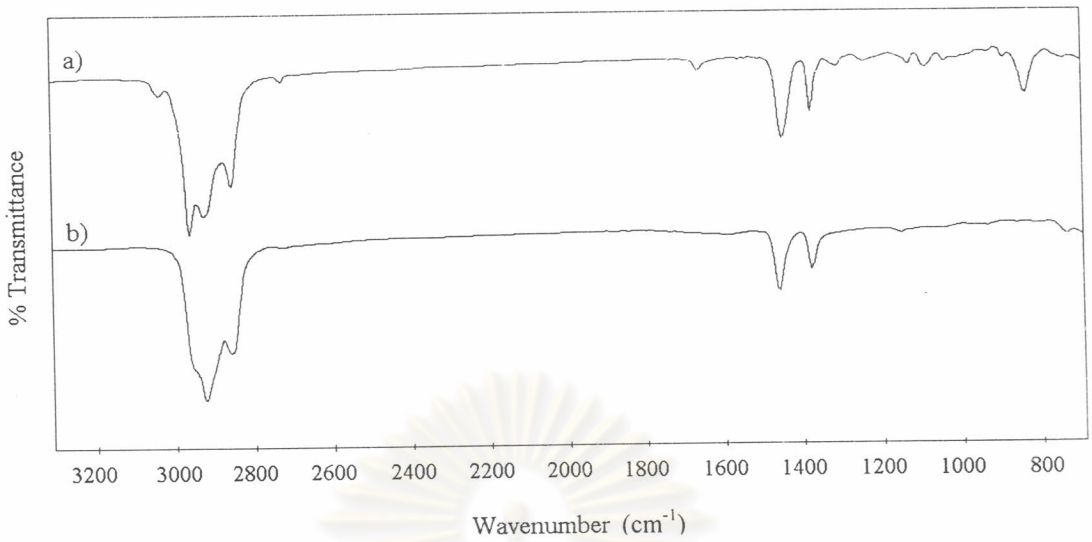

Figure 3.1: FTIR spectra of (a) CPIP, (b) HCPIP (97% hydrogenation), [Ru] = 200 μM; [C=C] = 260 mM; P_{H2} = 40.3 bar; T = 160°C.

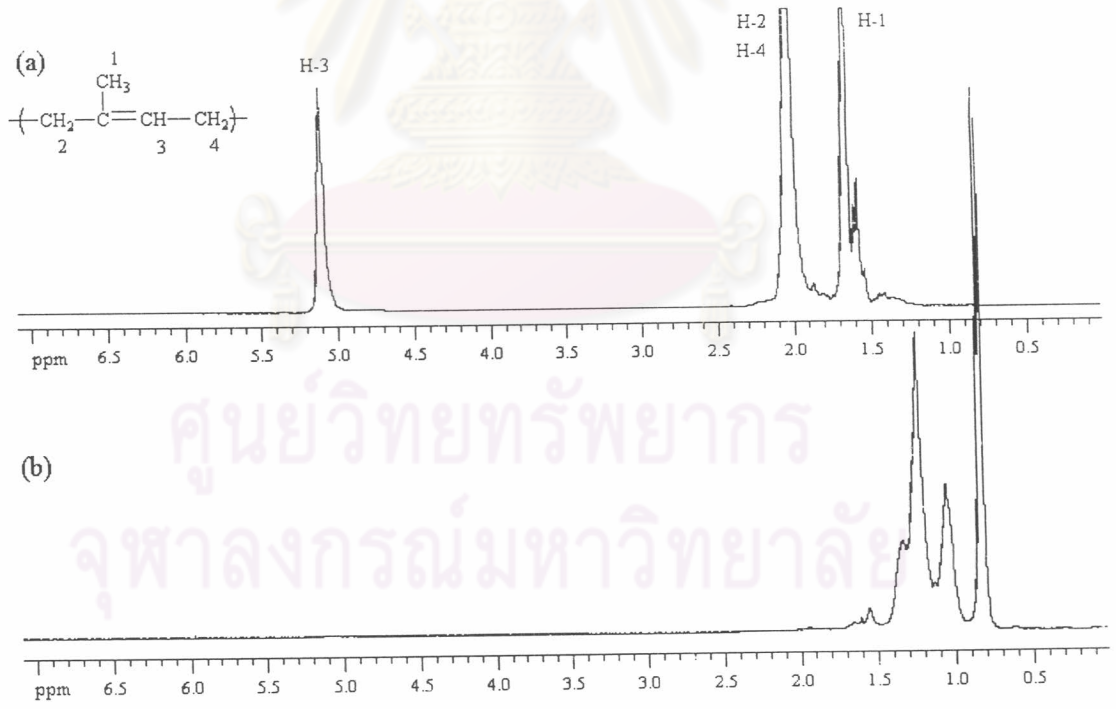

Figure 3.2: ^{1}H-NMR spectra of (a) CPIP, (b) HCPIP (97% hydrogenation), [Ru] = 200 μM; [C=C] = 260 mM; P_{H2} = 40.3 bar; T = 160°C.

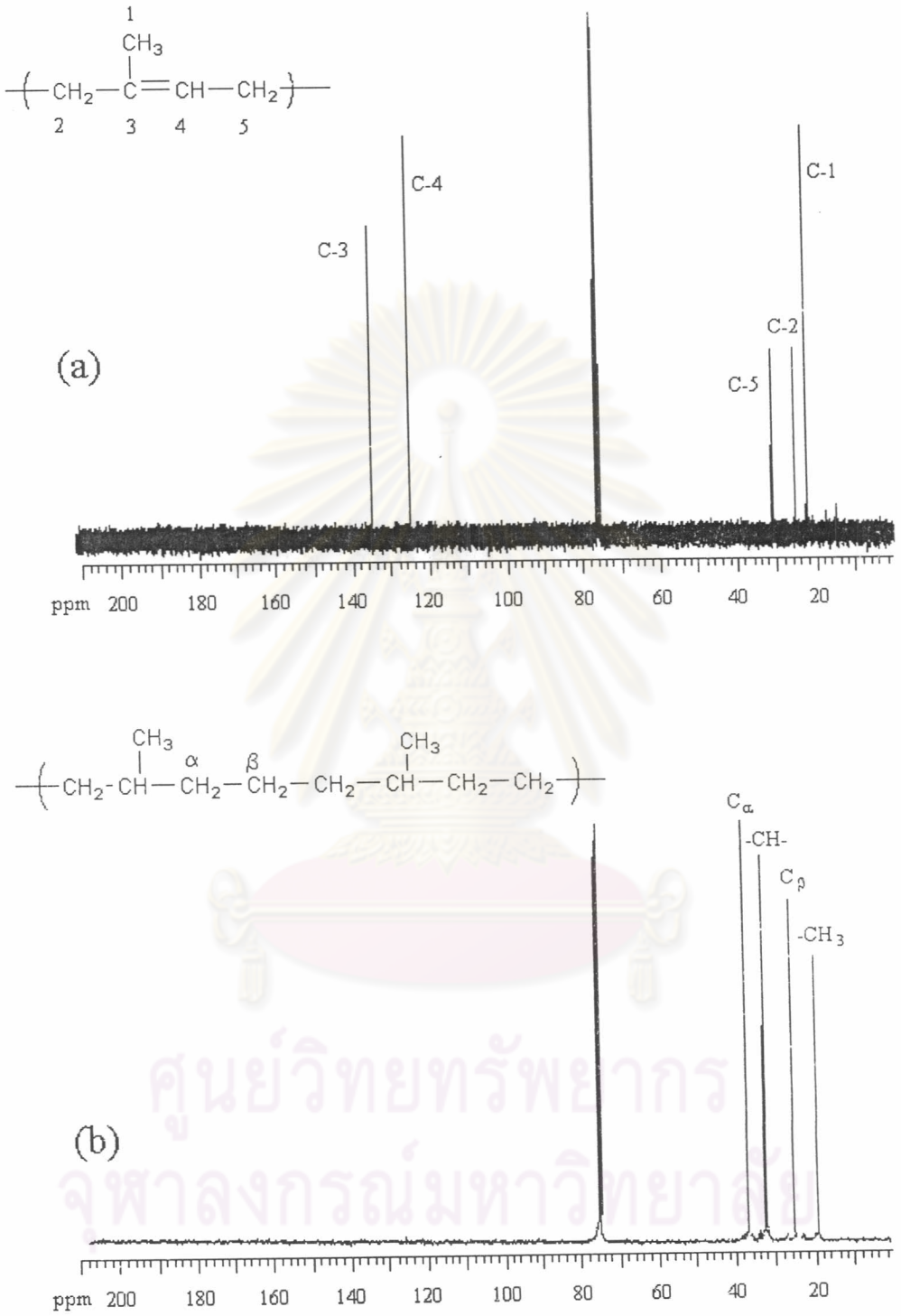

Figure 3.3: **^{13}C-NMR spectra of (a) CPIP, (b) HCPIP (97% hydrogenation), [Ru] = 200 μM; [C=C] = 260 mM; P_{H2} = 40.3 bar; T = 160°C.**

3.3 Kinetics of CPIP Hydrogenation Using $RuCl(CO)(CH=CHPh)(PCyH)_3)_2$

A kinetic study of CPIP hydrogenation in the presence of the homogeneous catalyst $Ru(CH=CH(Ph))Cl(CO)(PCy_3)_2$ was carried out using a computer controlled gas uptake apparatus to investigate the rate dependence of reaction variables, such as polymer concentration, catalyst concentration, temperature, and hydrogen pressure. Replicate experiments at the base set of conditions were performed periodically to ensure that the catalyst sample had not decomposed. The basic conditions were 160°C, $[C=C]_0$ = 260 mM (2.65 g CPIP), and $[Ru]_T$ = 200 μM (0.025 g) in 150 ml chlorobenzene solution. The base condition pressure was maintained by the gas uptake apparatus at 42.3 bar (600 psig) total pressure; the total pressure consisted of 40.3 bar (584.7 psia) hydrogen partial pressure and 2.0 bar (30 psia) chlorobenzene partial pressure.

A representative hydrogen uptake profile corresponding to the olefin consumption with respect to time is shown in Figure 3.4. All of the CPIP hydrogenation experiments are first order with respect to olefin concentration according to Equation 3.1 (where k′ is the pseudo first order rate constant).

$$-\frac{d[H_2]}{dt} = -\frac{d[C=C]}{dt} = k'[C=C] \qquad (3.1)$$

First order rate constants were calculated from the slope of the linear ln(1-x) versus time plots as shown in Figure 3.4 (where x is the conversion).

The functional relationship between the rate of reaction and concentration of polymer, catalyst, and hydrogen as well as temperature has been investigated by measuring the response of k′ to specific combination of factor levels. The rate constants derived from these experiments are tabulated in Table 3.2 and Table 3.4.

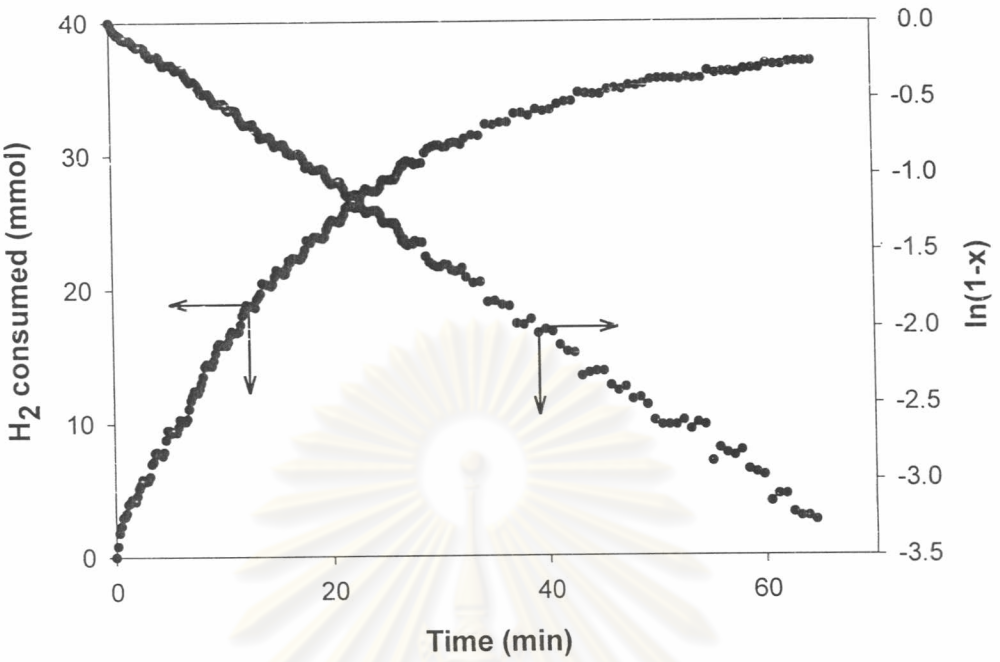

Figure 3.4: Hydrogen consumption plot for CPIP hydrogenation, [Ru] = 200 μM; [C=C] = 260 mM; P_{H2} = 40.3 bar; T = 160°C.

3.3.1 2^3 Factorial Design Experiments

To determine the significance of joint factor interactions, which influence the hydrogenation rate, a two-level factorial design was employed. Three principal factors, which are considered to have a main effect on the experimental rate constant (k′) are concentration of polymer, concentration of catalyst, and hydrogen pressure. For each variable, a low and high level was selected for the ranges of concentration to be examined. The range of polymer concentration, catalyst concentration, and hydrogen pressure were 130 – 520 mM, 100 – 200 μM, and 40.3 – 67.9 bar, respectively. In Table 3.2, the results for factorial design experiments are provided. An analysis of variance (ANOVA) of the rate constants is tabulated in Table 3.3. In this design, concentration of ruthenium and hydrogen pressure appear to be significant at the 95% confidence level. In contrast, the existence of two- and three-factor interaction effects is not statistically significant.

Table 3.2: 2^3 Factorial Design Data for CPIP Hydrogenation

Expt	[Ru] (μM)	[C=C] (mM)	P_{H2}[a] (bar)	$k' \times 10^3$ (s^{-1})	Relative Viscosity (η_{rel})
1	200	130	40.3	0.60	-
2	200	130	40.3	0.61	-
3	100	130	40.3	0.41	5.40
4	100	130	40.3	0.35	-
5	200	130	67.9	0.93	4.19
6	200	130	67.9	1.11	-
7	100	130	67.9	0.61	6.08
8	100	130	67.9	0.86	-
9	200	520	40.3	0.77	3.10
10	200	520	40.3	0.50	-
11	100	520	40.3	0.40	-
12	100	520	40.3	0.41	-
13	200	520	67.9	0.79	7.61
14	200	520	67.9	1.25	-
15	100	520	67.9	0.87	-
16	100	520	67.9	0.56	-

Conditions: T = 160°C; solvent was chlorobenzene. Volume = 150 ml

[a] partial pressure of H_2.

Table 3.3: Analysis of Variance (ANOVA) of 2^3 Factorial Experiments for Rate Constant (k′)

Source	Sum of Squares	DF	Mean Square	F	P[a]
[Ru]	3.02E-07	1	3.02E-07	17.643	0.0030
[C=C]	9.12E-09	1	9.12E-09	0.533	0.4862
P_{H2}	6.54E-07	1	6.54E-07	38.241	0.0003
[Ru]*[C=C]	9.92E-10	1	9.92E-10	0.058	0.8158
[Ru]*P_{H2}	8.46E-09	1	8.46E-09	0.495	0.5019
[C=C]*P_{H2}	1.22E-09	1	1.22E-09	0.072	0.7958
[Ru]*[C=C]*P_{H2}	1.16E-09	1	1.16E-09	0.068	0.8015
Error	1.37E-07	8	1.71E-08		
Total	9.15E-06	16			
Corrected Total	1.11E-06	15			

[a] if $P > 0.05$, then the variable is not significant.

From these results, univariate experiments were formulated and performed. The influence of each factor on the hydrogenation reaction; i.e., polymer concentration, catalyst concentration, hydrogen pressure, and temperature was also explored. The results of these trials are provided in Table 3.4 and will be subsequently discussed.

3.3.2 Effect of Ruthenium Concentration

The dependence of the initial hydrogenation rate on catalyst concentration was studied over the range of 20 - 250 μM (2.5 – 31.2 mg in 150 mL chlorobenzene) at 160°C. The concentration of initial C=C unsaturation was 260 mM under 40.3 bar hydrogen pressure. The conversion profiles at a variety of catalyst concentrations (Figure 3.5a) indicate that above the 40 μM catalyst concentration the system displays the expected first order behavior with respect to olefin concentration. The reaction rate is linearly proportional to the total concentration of catalyst as shown in Figure 3.5b. This is consistent with the investigations of Martin et al. (1997) for NBR hydrogenation catalyzed by $Ru(CH=CH(Ph))Cl(CO)(PCy_3)_2$ and Charmondusit et al. (2003) for CPIP hydrogenation catalyzed by $OsHCl(CO)(O_2)(PCy_3)_2$. The first order response of k′ dependence on the total ruthenium concentration confirmed that the active complex is a mononuclear species.

Table 3.4: Summary of Kinetic Data from the Study of CPIP Hydrogenation Catalyzed by $Ru(CH{=}CH(Ph))Cl(CO)(PCy_3)_2$

Expt	[Ru]	$[C{=}C]_0$	P_{H2}[a]	Temp	$k'x10^3$	Hydrogenation		Relative Viscosity
						%	Time	
	(μM)	(mM)	(bar)	(°C)	(s^{-1})		(h)	(η_{rel})
1	20	260	40.3	160	0.11	42.3	4.1	-
2	40	260	40.3	160	0.24	70.2	3.4	-
3	80	260	40.3	160	0.31	91.7	3.3	-
4	100	260	40.3	160	0.41	96.8	2.8	5.28
5	130	260	40.3	160	0.48	96.8	2.4	-
6	170	260	40.3	160	0.51	98.1	1.8	5.66
7	200	260	40.3	160	0.62	96.7	2.0	5.10
8	250	260	40.3	160	0.80	99.5	1.5	-
9	200	260	5.9	160	0.04	35.0	3.1	-
10	200	260	12.8	160	0.10	71.4	4.0	-
11	200	260	19.7	160	0.19	82.2	3.0	4.11
12	200	260	26.6	160	0.28	96.8	3.2	5.31
13	200	260	33.5	160	0.50	98.8	2.2	4.84
14	200	260	40.3	160	1.02	99.6	1.9	2.41
15	200	130	40.3	160	0.60	96.4	1.5	-
16	200	130	40.3	160	0.60	99.0	1.6	-
17	200	520	40.3	160	0.77	98.2	1.6	3.10
18	200	520	40.3	160	0.50	91.8	2.3	-
19	200	130	67.9	160	0.93	97.5	1.0	4.19
20	200	130	67.9	160	1.11	98.1	1.2	-
21	200	520	67.9	160	1.25	95.5	1.1	-
22	200	520	67.9	160	0.99	90.5	2.3	7.61
23	100	130	40.3	160	0.41	95.5	2.0	5.40
24	100	130	40.3	160	0.35	96.7	2.1	-
25	100	520	40.3	160	0.40	91.5	1.9	-
26	100	520	40.3	160	0.41	75.4	2.2	-
27	200	260	40.3	130	0.18	79.4	4.1	-
28	200	260	40.3	140	0.34	98.8	2.9	2.98
29	200	260	40.3	150	0.41	97.2	1.2	3.82
30	200	260	40.3	170	0.83	94.6	2.1	-
31	200	260	40.3	180	1.05	97.4	1.5	-
32	200	130	40.3	130	0.18	93.8	3.9	-
33	200	130	40.3	140	0.33	92.5	2.1	4.30
34	200	130	40.3	150	0.35	95.6	2.3	3.23
35	200	130	40.3	160	0.61	98.9	1.9	-
36	200	130	40.3	170	0.80	98.9	1.7	2.44
37	200	130	40.3	180	0.94	95.3	1.0	4.41

Solvent = chlorobenzene. Volume = 150 ml

[a] partial pressure of H_2.

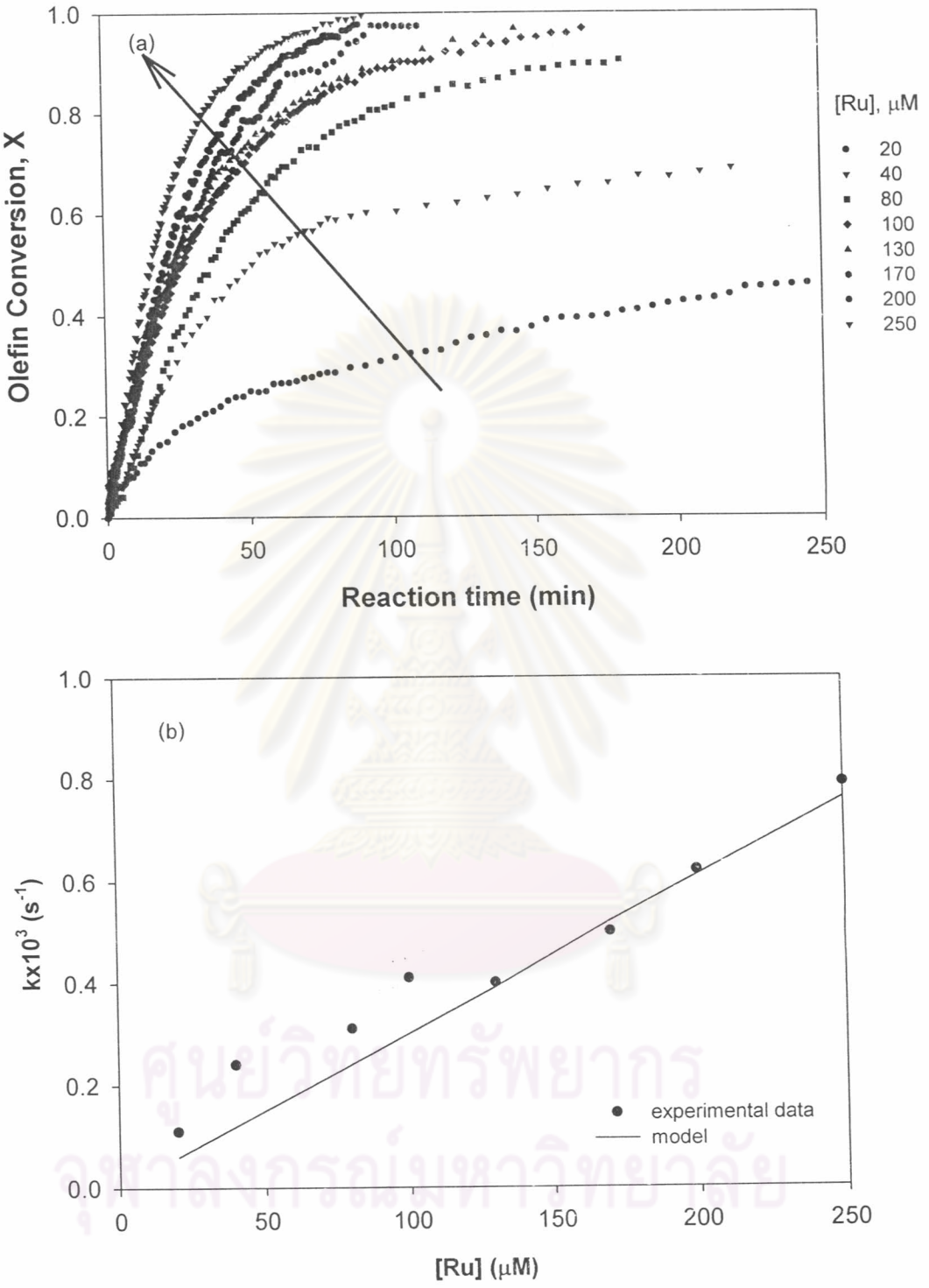

Figure 3.5: (a) Effect of [Ru] on CPIP conversion profiles, (b) Effect of [Ru] on rate constant. [C=C] = 260 mM; P_{H2} = 40.3 bar; T = 160°C.

3.3.3 Effect of Hydrogen Pressure

Martin et al. (1997) has previously suggested the estimation of accurate values of hydrogen pressure in the reactor. The partial pressure of chlorobenzene was approximated based on the Harlacher - Braun correlation, assuming that the polymer concentration and hydrogen pressure did not significantly affect the vapor pressure (Reid et al., 1977). The actual vapor pressure measured by using the gas uptake apparatus in the absence of hydrogen at 160°C, was 0.204 MPa.

A series of experiments in which the hydrogen pressure was varied over the range of 5.9 to 67.9 bar was carried out. The initial concentration of polymer and catalyst were kept at 260 mM and 200 μM, respectively at 160°C in chlorobenzene. The conversion versus time plots for different hydrogen pressures as shown in Figure 3.6a indicate that the expected first order behavior with respect to olefin concentration is observed, above 5.9 bar hydrogen pressure. Figure 3.6b illustrates the first order rate dependence on hydrogen pressure over the experimental range investigated. This first order behavior implied that a single mechanistic pathway is probably involved in the reaction of the polymer with hydrogen. These results are in agreement with those for NBR hydrogenation in the presence of the $Ru(CH=CH(Ph))Cl(CO)(PCy_3)_2$ catalyst system (Martin et al., 1977), whereas, the hydrogenation of NBR (Parent et al., 1998) and CPIP (Charmondusit et al., 2003) using the osmium complex, $OsHCl(CO)(O_2)(PCy_3)_2$ was known to shift from second order to zero order dependence on hydrogen with increasing hydrogen pressure.

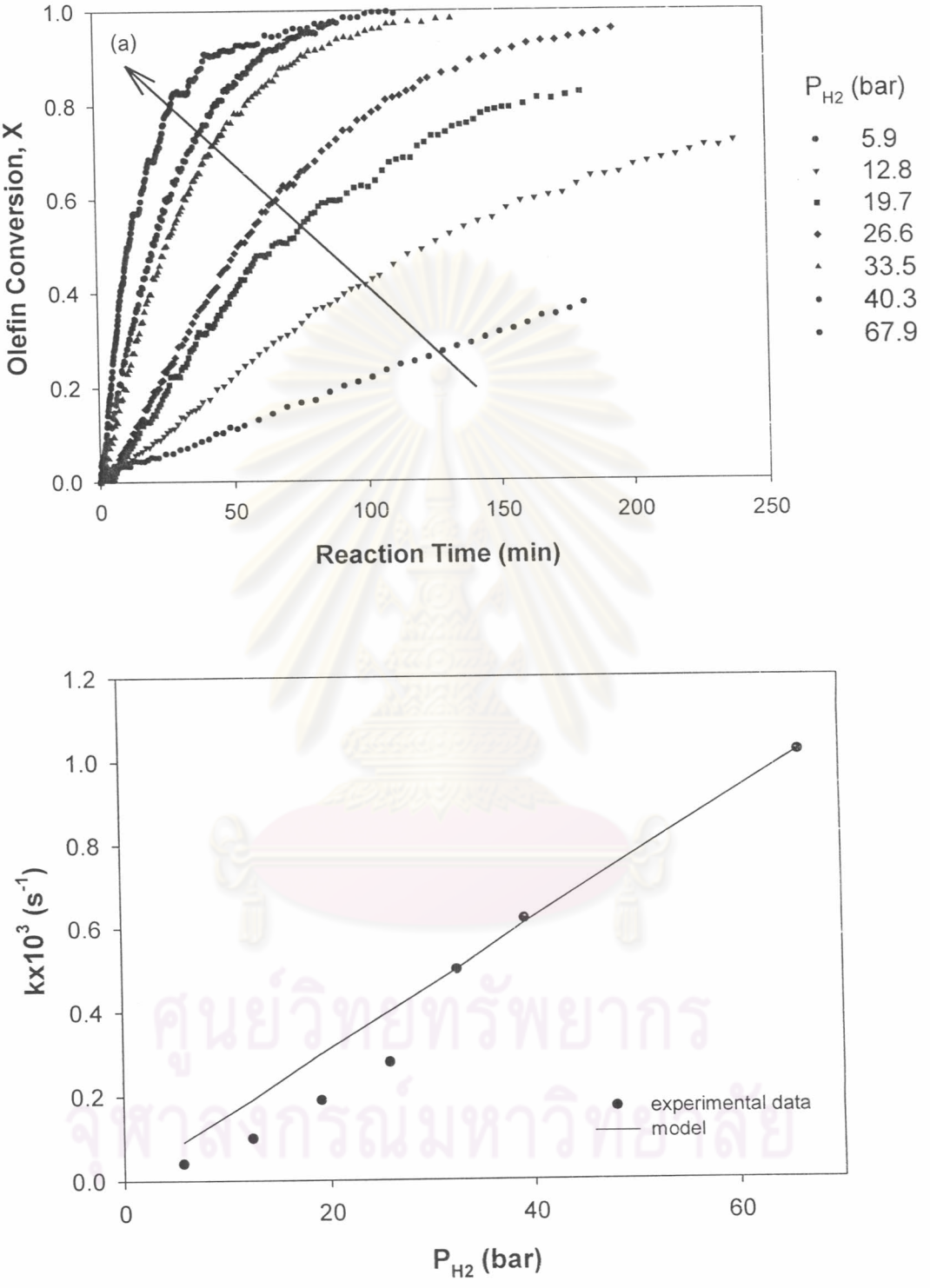

Figure 3.6 : (a) Effect of P_{H2} on CPIP conversion profiles, (b) Effect of P_{H2} on rate constant. [C=C] = 260 mM; [Ru] = 200 μM; T = 160°C.

3.3.4 Effect of Double Bond Concentration

As mentioned above, the conversion profile for hydrogenation of CPIP is pseudo first order with respect to [C=C] and is independent of the amount of olefin charged to the reactor. This behavior was observed at all sets of carbon - carbon double bond concentrations and reaction conditions employed as shown by the results obtained for the factorial design experiments and univariate studies. The plot of initial reaction rate versus polymer concentration in Figure 3.7 clearly shows that the reaction rate constants remain relatively unchanged over the range of polymer concentration studied (130 – 520 mM) at 160°C in chlorobenzene. For NBR hydrogenation catalyzed by $Ru(CH=CH(Ph))Cl(CO)(PCy_3)_2$ (Martin et al., 1977) and $OsHCl(CO)(O_2)(PCy_3)_2$ (Parent et al., 1998), the rate constants show an inverse dependence on nitrile concentration due to competitive complexation of nitrile to the active catalyst site. Consequently, the NBR hydrogenation activity decreased as the amount of polymer concentration increases.

3.3.5 Effect of Added Tricyclohexylphosphine

The dependence of the initial hydrogenation rate on the addition of tricyclohexylphosphine (PCy_3) was investigated to understand the function of PCy_3 ligand in the catalytic mechanism. The values of the experimental rate constant along with the concentration of added PCy_3 are presented in Figure 3.8 and Table 3.5. Amounts ranging from 0 to 6.6 equivalents (6.6 times the number of moles of catalyst in the reactor) of tricyclohexylphosphine were used. It is evident that adding tricyclohexylphosphine retards the potential activity of the ruthenium complexes for hydrogenation. This result may be explained by either of two mechanisms; the competitive coordination of PCy_3 with the active catalyst species (Equation 3.2) or the inhibition of phosphine dissociation from ruthenium hydride species (Equation 3.3) (Martin et al., 1997).

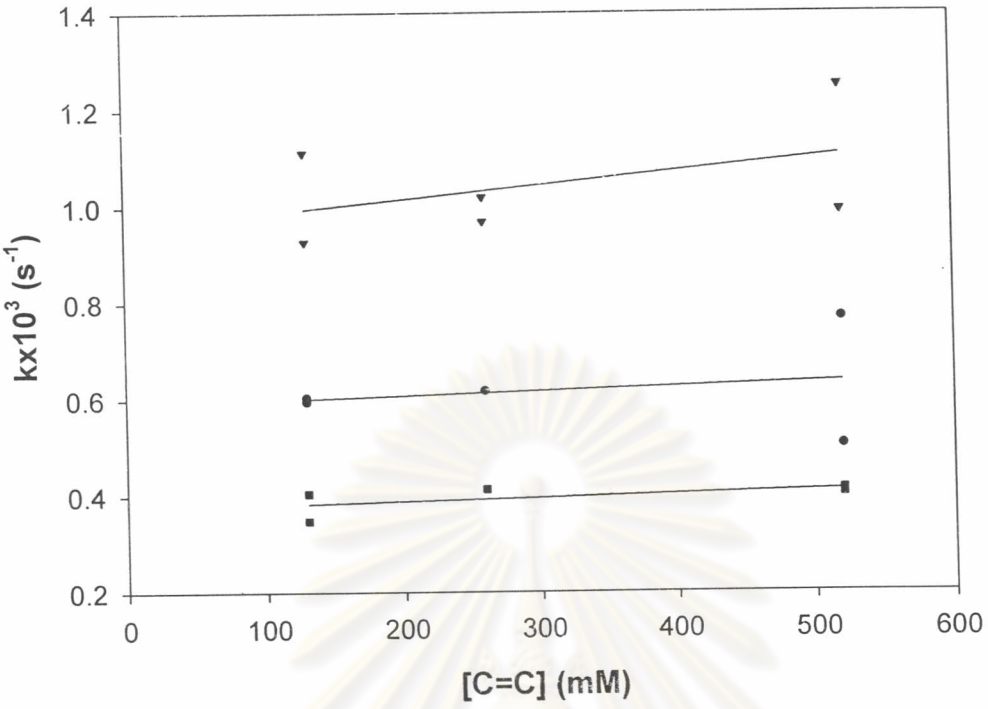

Figure 3.7: Effect of [C=C] on rate constant for CPIP hydrogenation, T = 160°C. (●) P_{H2} = 40.3 bar; [Ru] = 200 μM, (▼) P_{H2} = 67.9 bar; [Ru] = 200 μM, (■) P_{H2} = 40.3 bar; [Ru] = 100 μM.

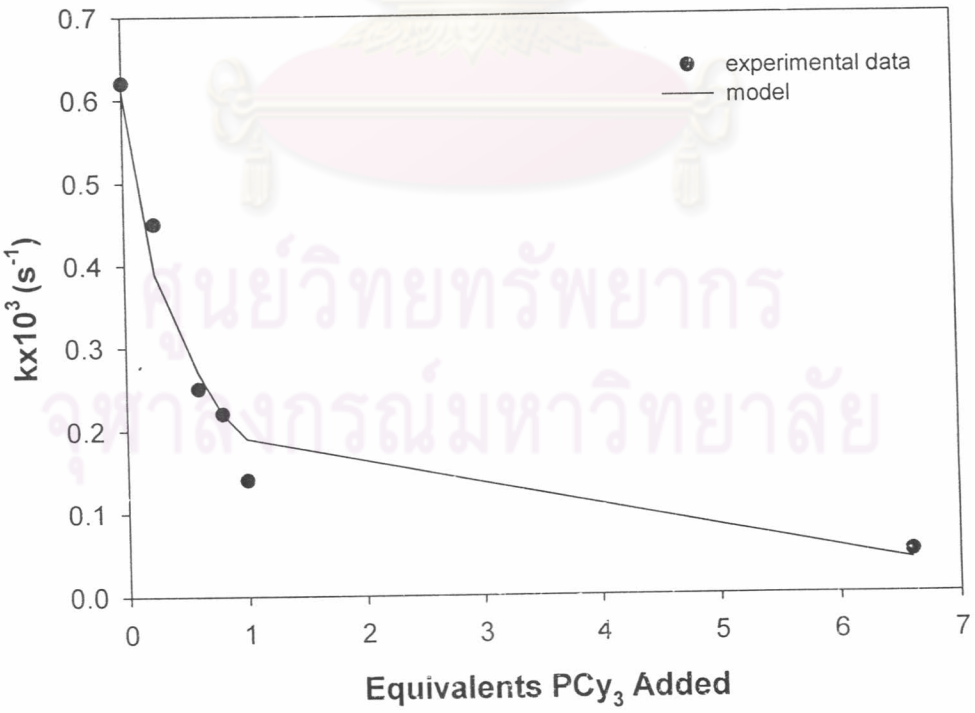

Figure 3.8: Effect of added PCy_3 on rate constant. [C=C] = 260 mM; P_{H2} = 40.3 bar; [Ru] = 200 μM; T = 160°C.

$$RuHCl(CO)(PCy_3)_2 + PCy_3 \overset{K_a}{\rightleftharpoons} RuHCl(CO)(PCy_3)_3 \quad (3.2)$$

$$RuHCl(CO)(PCy_3)_2 \overset{K_d}{\rightleftharpoons} RuHCl(CO)(PCy_3) + PCy_3 \quad (3.3)$$

One possible reason for the severity of the catalytic inhibition by PCy_3 involved the formation of a complex between the free tricyclohexylphosphine and the hydride catalyst. This is evident by ^{31}P-NMR spectrum, showing a new phosphorous species at 46.7 ppm when a solution of the hydride and some free PCy_3 in deoxygenated C_6D_6/toluene was examined. It can be implied that the formation of the tri-phosphine complex $RuHCl(CO)(PCy_3)_3$ seems possible, although it is sterically crowded (Martin, 1991).

Another possible explanation for the inverse dependence was that the dissociation of PCy_3 from the hydride catalyst generative a monophosphine complex which could enter into the catalytic cycle. The dissociation experiment performed by dissolving a sample of the hydride catalyst in deoxygenated C_6D_6/toluene at 70°C demonstrated no evidence of a monophosphine complex, which can be attributed to Equation 3.3. However, it is certain that coordinated PCy_3 is labile as it undergoes exchange with free phosphine in solution. Tentative NMR evidence indicates this exchange process could be dissociative in nature, suggesting that a monophosphine transition state may be generated in trace quantities. Small amount of free phosphine would inhibit the formation of the active species, thereby reducing the observed activity. This is considered to be the most plausible explanation for the PCy_3 inhibition effect (Parent et al., 1998).

In support of PCy_3 dissociation mechanism, supplementary experiments using $RuHCl(CO)(PPr^i_3)_2$, which PPr^i_3 is less steric than PCy_3 and a smaller phosphine of similar electron-donating capacity, proved to be less active than the cyclohexyl analogue, $RuHCl(CO)(PCy_3)_2$ (Section 3.2) The inferior CPIP hydrogenation rate in the presence of $RuHCl(CO)(PPr^i_3)_2$ could be expected when the formation of an active center to be initiated by PPr^i_3 dissociation. Therefore, a phosphine dissociation step may be incorporated in the hydrogenation mechanism.

Table 3.5: Effect of PCy_3 Addition and Solvent on the Hydrogenation of CPIP

Solvent	equivalents of added PCy_3	$k' \times 10^3$ (s^{-1})
Xylene	0	0.37
Toluene	0	0.50
Chlorobenzene	0	0.61
Chlorobenzene	0.25	0.45
Chlorobenzene	0.6	0.25
Chlorobenzene	0.8	0.22
Chlorobenzene	1	0.14
Chlorobenzene	6	0.05

Conditions: P_{H2} = 40.3 bar; T = 160°C; [Ru] = 200 μM; [C=C] = 260 mM.

3.3.6 Effect of Solvent

The hydrogenation of CPIP was also carried out using various solvents at 160°C and 40.3 bar P_{H2} in the presence of 200 μM [Ru], and 260 mM [C=C]. Ketone solvents such as acetone and methyl ethyl ketone were not employed as the solvent for CPIP hydrogenation, since polyisoprene does not dissolve in these polar solvents. Table 3.5 summarizes the results of CPIP hydrogenation catalyzed by Ru(II) complex in various solvents. The rate of hydrogenation of CPIP increases in the order: chlorobenzene > toluene > xylene. The use of chlorinated solvent results in a faster reaction rate than in any of the other solvents investigated. Therefore, it seems that the more polar solvent, the higher rate of reduction. This may be due to the solvent interaction with the polymer in promoting active site availability and the nature of solvated ruthenium hydride.

3.3.7 Effect of Temperature

Two sets of experiments were carried out over the temperature range of 130 to 180°C, where hydrogen pressure (40.3 bar) and total ruthenium concentration (260 μ M) remained constant. The first set investigated the effect of varying temperature using polymer concentration of 260 mM, whereas a concentration of carbon - carbon double bond of 130 mM was used in the second set. The experimental observations are listed in Table 3.4 and the corresponding Arrhenius plot is shown in Figure 3.9a.

Linear responses for both sets of experiments are observed, from which an apparent activation energy is estimated to be 51.1 kJ/mol over the temperature range

of 130 to 180°C. The rates of hydrogenation of CPIP for this ruthenium catalyst are very much slower than the rate of CPIP hydrogenation in toluene catalyzed by OsHCl $(CO)(O_2)(PCy_3)_2$ for which the activation energy was 109.3 kJ/mol over the temperature range of 115 to 140°C (Charmondusit et al., 2003). However, the apparent activation energy of 51.1 kJ/mol is still indicative that the experiments were carried out under chemical control without mass transfer limitation. Furthermore, these experiments also confirmed that the rate constant is independent on polymer concentration. Based on the corresponding Eyring equation (Equation 3.4), the apparent activation enthalpy and entropy estimated are 47.6 kJ/mol and –197.2 J/mol K, respectively as shown in Figure 3.9b.

$$k = \frac{k_B T}{h} e^{\frac{-\Delta H^+}{RT}} e^{\frac{\Delta S^+}{R}} \qquad (3.4)$$

where k_B = Boltzmann's constant = 0.381×10^{-23} J · K^{-1}

h = Plank's constant = 6.626×10^{-34} J · s

3.3.8 Effect of Polymer Purification

To study the effect of polymer purity on hydrogenation, CPIP was purified by dissolving in chlorobenzene and then reprecipitating with ethanol. The polymer was dried under vacuum for a week to remove the trapped solvent. To ensure that no more solvent was left in the sample, the mass of polymer was periodically recorded. The sample was re-dissolved again in chlorobenzene and hydrogenated under the base condition (P_{H2} = 40.3 bar, T = 160°C, [Ru] = 200 μM, [C=C] = 260 mM, chlorobenzene). The pseudo first order reaction rate constant of purified CPIP (6.55×10^{-4} s^{-1}) was insignificantly higher than that of unpurified CPIP (6.10×10^{-4} s^{-1}) at base condition. The slight increase in rate constant may be due to trace polymer contaminants such as chain transfer agents, which are likely removed by solvent extraction and coagulation.

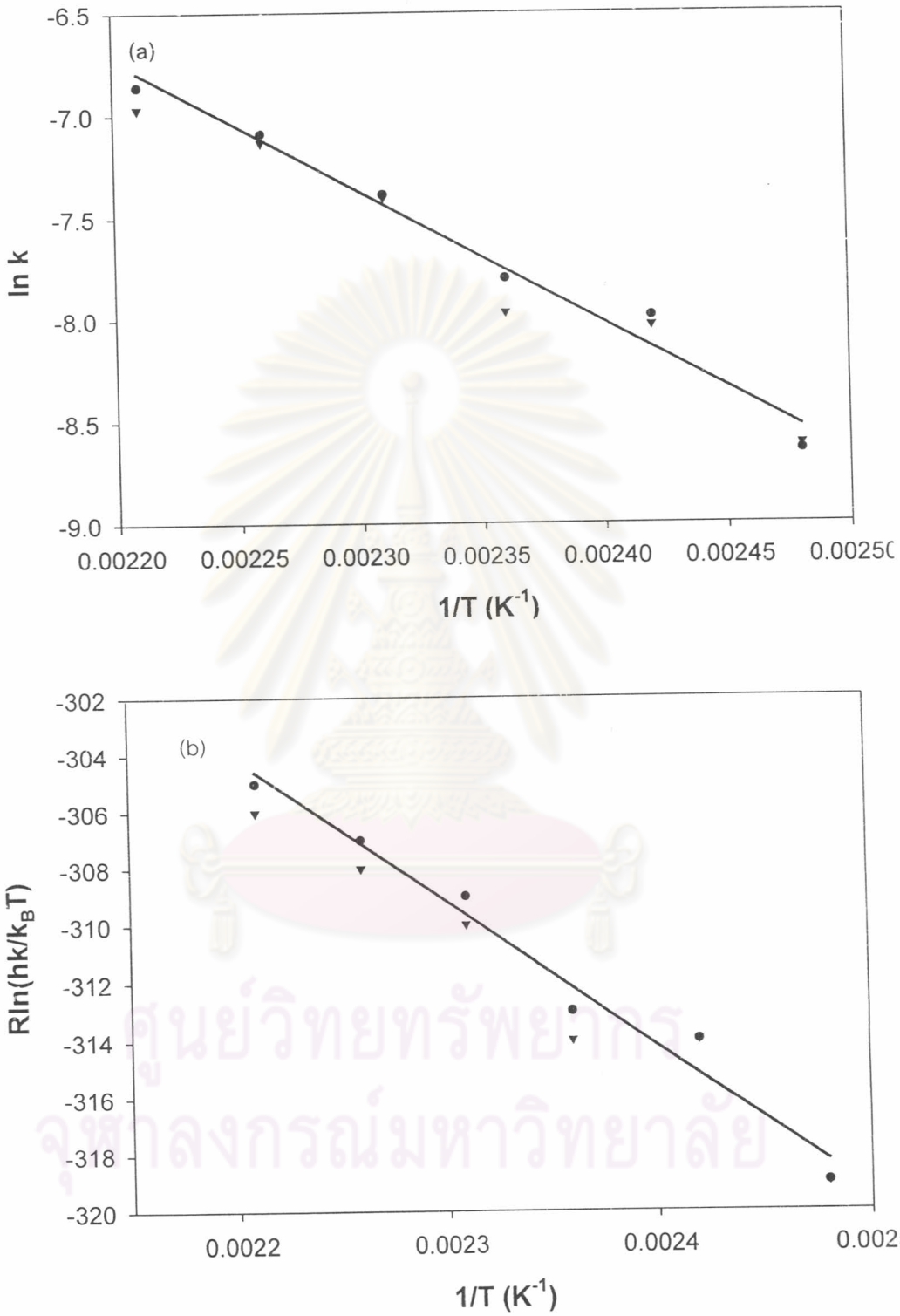

Figure 3.9: (a) Arrhenius plot, (b) Eyring plot for CPIP hydrogenation, [Ru] = 200 μM; T =160°C; P_{H2} = 40.3 bar. (▼) [C=C] = 130 mM, (◆) [C=C] = 260 mM.

3.3.9 Effect of Acid Addition

Yi et al. (2000) revealed a way to increase the catalyst activity of alkene hydrogenation. The method for selectively promoting the dissociation and trapping PCy_3 ligands in $RuHCl(CO)(PCy_3)_2$ catalyst and generating a highly reactive 14-electron monophosphine ruthenium complex has been developed by using acid. Since phosphine dissociation is suspected in the hydrogenation of CPIP cycle (section 3.3.2.5) acid-promoted hydrogenation was investigated. Table 3.6 presents the effect of acid addition on hydrogenation of CPIP. As little as 4 mole equivalent (4 times the number of mole of catalyst in the reactor) of acid added to the system had a dramatic effect on the catalyst activity. Among the selected group of acids, *p*-toluenesulfonic acid (*p*-TsOH) was found to be the most efficient promoter for CPIP hydrogenation (98.3 % hydrogenation in 1.5 hours), since sulfonic acids are more acidic than carboxylic acids. These results suggested that the strong acid promotes the hydrogenation rate by selective entrapment of the phosphine ligand more than the weak acid in the order: *p*-TsOH > 3-chloropropionic acid > succinic acid. The optimum amount of *p*-TsOH affording the highest reaction rate was a 22 equivalents. The extent of hydrogenation does not change with the increase in *p*-TsOH amount.

Table 3.6: Effect of Acids Addition on CPIP Hydrogenation

Acid	Equivalents of added acid[a]	% Hydrogenation	Reaction Time (h)
-	0.0	93.0	5.0
succinic acid	7.0	89.9	2.0
3-chloropropionic acid	7.7	96.7	2.0
p-toluenesulfonic acid	4.4	98.3	1.5
p-toluenesulfonic acid	8.8	99.7	1.5
p-toluenesulfonic acid	11.0	99.6	1.5
p-toluenesulfonic acid	13.2	99.5	1.5
p-toluenesulfonic acid	22.0	98.5	1.5

Condition: P_{H2} = 40.3 bar, Temp = 160°C, [Ru] = 200μM, [C=C] = 260mM. solvent = chlorobenzene.

[a] 1 equivalent = 0.87 millimole

3.4 Polymer Chain Length Properties

IR and NMR spectroscopies were used to confirm the degree of hydrogenation indicated from the gas consumption experiments. However, these techniques lack the sensitivity required to detect the presence of side reactions such as crosslinking and chain scission. Therefore, the relative viscosity (η_{rel}) measurement of a dilute polymer solution with pure toluene was undertaken to investigate the effect of side reactions on the CPIP hydrogenation using $Ru(CH=CH(Ph))Cl(CO)(PCy_3)_2$.

The η_{rel} measurement of some hydrogenated CPIP products is also presented in Table 3.2 and Table 3.4. The effect of catalyst concentration, C=C concentration and hydrogen pressure on the relative viscosity of hydrogenated CPIP is illustrated in Figure 3.10a - c. It can be seen that relative viscosity of CPIP ($\eta_{rel} \sim 9$) is higher than that of hydrogenated CPIP ($\eta_{rel} \sim 2$-6). The reduction of HCPIP relative viscosity indicates that chain scission occurred during the catalytic hydrogenation of CPIP. The random viscosity shows that the reaction conditions employed have insignificant effect on the product properties. These results are different from those observed for the hydrogenation of CPIP using $OsHCl(CO)(O_2)(PCy_3)_2$ at 130°C and 6.9 - 69 bar P_{H2} in which no degradation and/or crosslinking occurred during the hydrogenation process (Charmondusit et al., 2003). This may be due to the fact that the hydrogenation catalyzed by ruthenium based catalysts was performed at higher temperature and higher pressure.

Molecular weight reduction was also confirmed by the results from gel permeation chromatography. Table 3.7 shows the decrease in polymer chain length during hydrogenation. Number average molecular weight (Mn = 150000 – 450000) and weight average molecular weight (Mw = 250000 – 650000) of hydrogenated CPIP is substantially lower than for the parent polymer (Mn = 9570000 and Mw = 1270000). Furthermore, polydispersity was somewhat altered during the hydrogenation reaction (Figure 3.11a). One can also notice that treatment of CPIP under the standard hydrogenation condition without the ruthenium complex for 24 hours results in a decrease in molecular weight of CPIP (Mn = 285000 and Mw = 444000) compared to the molecular weight of the starting polymer (Figure 3.11b and Table 3.7). This suggests that the high temperature and pressure used during the reaction caused main molecular chain scission of the polymer.

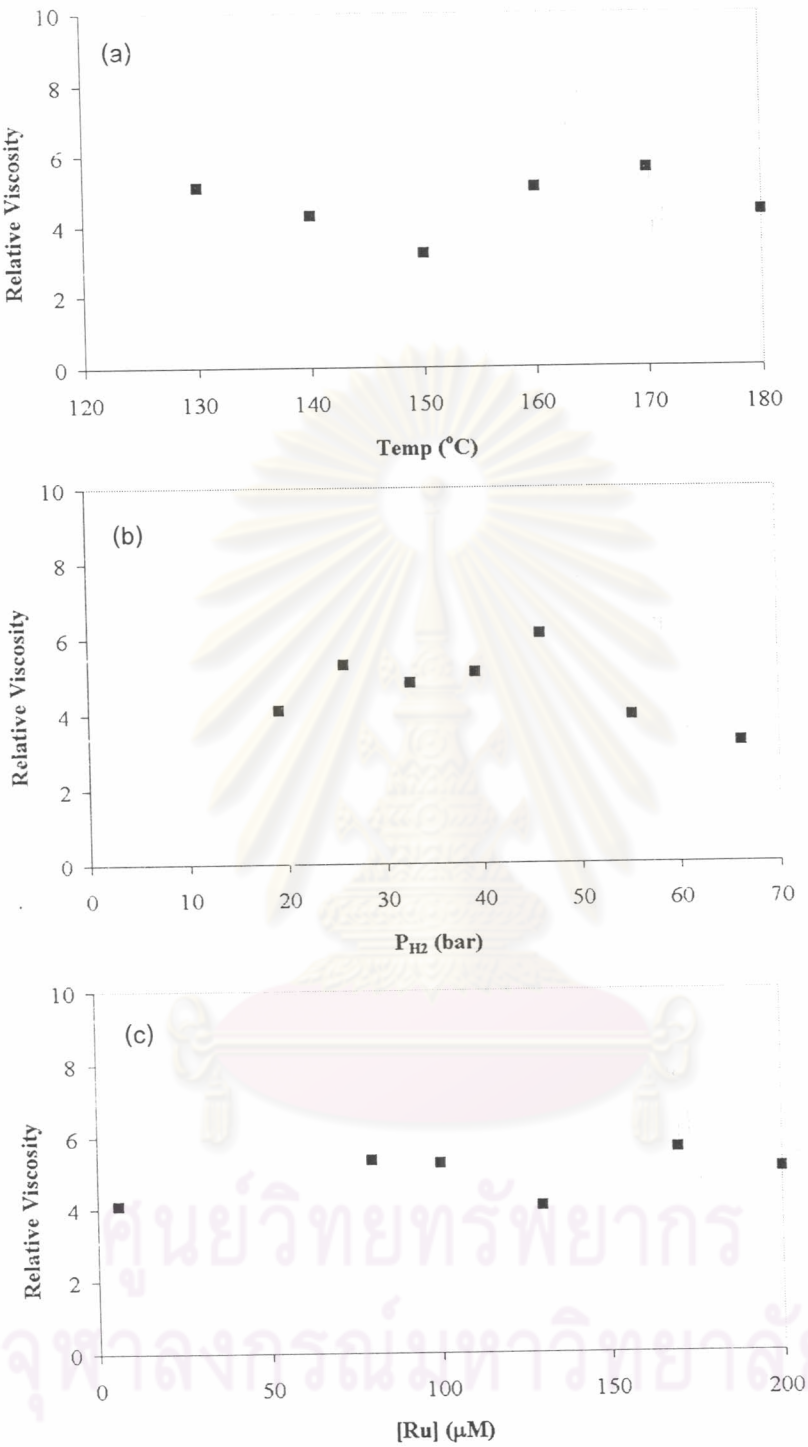

Figure 3.10: (a) Relative viscosity of HCPIP versus temperature, [C=C] = 260 mM; [Ru] = 260 μM; P_{H2} = 40.3 bar.
(b) Relative viscosity of HCPIP versus pressure, [C=C] = 260 mM; [Ru] = 260 μM; T = 160°C.
(c) Relative viscosity of HCPIP versus ruthenium concentration, [C=C] = 260 mM; P_{H2} = 40.3 bar; T = 160°C.

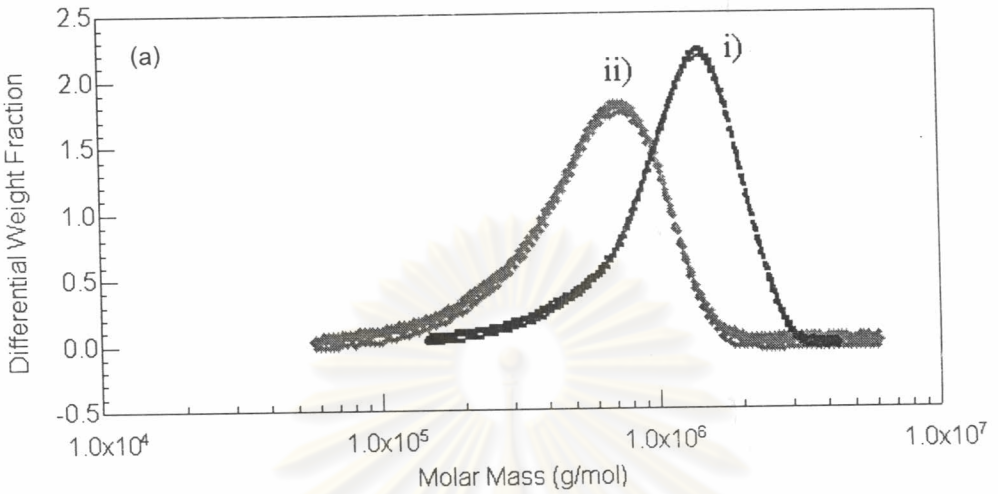

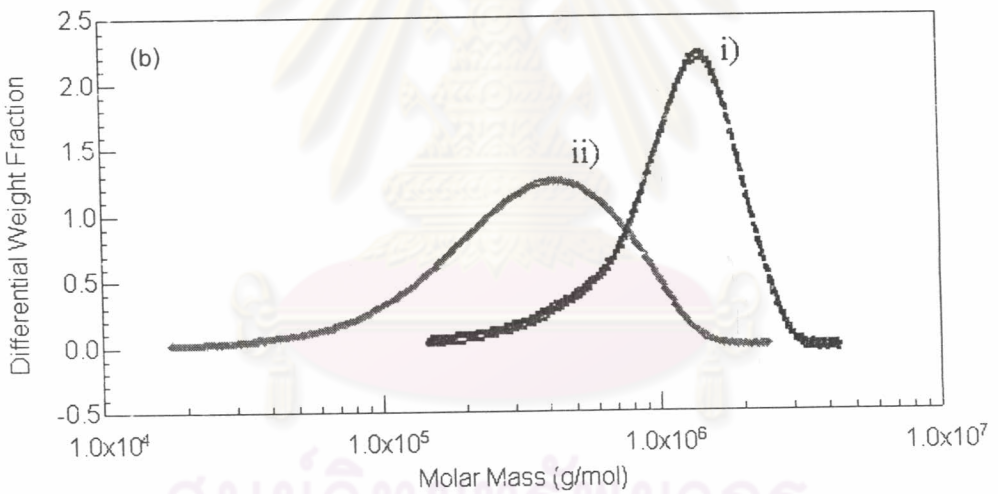

Figure 3.11: (a) Gel permeation chromatograms of (i) CPIP and (ii) HCPIP (97% hydrogenation). [Ru] = 200 μM; [C=C] = 260 mM; P_{H2} = 40.3 bar; T = 160°C.
(b) Gel permeation chromatograms of (i) CPIP and (ii) CPIP reaction without Ru catalyst. [C=C] = 260 mM; P_{H2} = 40.3 bar; T = 160°C for 24 h.

Table 3.7: Summary of GPC Molecular Weight Data for CPIP and HCPIP

Polymer	Condition				Mn	Mw	Polydispersity
	[C=C] (mM)	Temp (^{o}C)	P_{H2} (bar)	[Ru] (μM)			
CPIP	-	-	-	-	956800	1274000	1.33
CPIP[a]	260	160	40.3	-	284600	443600	1.56
HCPIP	260	160	40.3	200	441000	616500	1.40
HCPIP	130	160	40.3	200	447400	658200	1.47
HCPIP	130	160	67.9	200	331700	536200	1.62
HCPIP	520	160	26.6	200	152900	257300	1.68
HCPIP	260	150	40.3	200	372600	557900	1.50
HCPIP	260	130	40.3	200	307200	470400	1.53

[a] CPIP reaction was carried out under this condition for 24 h.

3.5 Reaction Mechanism and Statistical Analysis

The hydrogenation of CPIP followed pseudo first order kinetics with respect to the concentration of carbon - carbon double bond from 0 to over 90% conversion. Therefore, the pseudo first order rate constant that obtained from the gas uptake data had a single value throughout the reaction, in spite of the change in double bond concentration. Based on the kinetic data, the hydrogenation was found to be first order with respect to the total concentration of ruthenium and hydrogen and inverse order in the concentration of added tricyclohexylphosphine over the range of studies. The rationalization of the inverse dependence of rate constant on the amount of added PCy_3 was interpreted in term of two mechanisms; the competitive coordination of PCy_3 and the inhibition of PCy_3 dissociation (section 3.3.2.5). However, the result of competitive complexation of the ligand with the active species in the reaction mixture was not considered in the mechanism due to severe steric crowding. All of the kinetic dependence experiments were performed without added ligands. Thus, the rate law of CPIP hydrogenation may be summarized as follows:

$$k' = \frac{k[Ru]_T P_{H_2}}{(\alpha + \beta[PCy_3])} \qquad (3.5)$$

It seems likely that the five coordinate complex, 16 electron hydride catalyst $RuHCl(CO)(PCy_3)_2$ is rapidly formed from the styryl catalyst, Ru(CH=CH(Ph))Cl

$(CO)(PCy_3)_2$ in the presence of H_2. Moreover, the styryl and the hydride catalyst show same catalytic activity, suggesting that both catalysts may share the same catalytic active species.

The mechanism illustrated in Figure 3.12 is proposed as the most significant pathway for hydrogenation of CPIP. The first stage in the hydrogenation process is rapid hydrogenation of the styryl group in $Ru(CH=CH(Ph))Cl(CO)(PCy_3)_2$ to give ruthenium hydride $RuHCl(CO)(PCy_3)_2$ and ethyl benzene (Equation 3.6). The mole ratio of the uptake hydrogen to the catalyst is 2:1, this confirms that for the present system Equation 3.6 is a fast equilibrium and lies far to the right. Under a hydrogen atmosphere, the hydride complex, $RuHCl(CO)(PCy_3)_2$ likely dissociates a phosphine ligand according to Equation 3.7 to give the intermediate $RuHCl(CO)(PCy_3)$.

$$Ru(CH=CH(Ph))Cl(CO)(PCy_3)_2 + 2H_2 \rightarrow RuHCl(CO)(PCy_3)_2 + CH_3CH_2(Ph) \quad (3.6)$$

$$RuHCl(CO)(PCy_3)_2 \overset{K_1}{\rightleftharpoons} RuHCl(CO)(PCy_3) + PCy_3 \quad (3.7)$$

The absence of a deuterium isotope effect indicates that the rate determining step of the cycle involves the coordination of olefin (Martin et al., 1997). This implied that the next step of the reaction path would be the coordination of H_2 to the monophosphine complex, $RuHCl(CO)(PCy_3)$, (Equation 3.8). This would be followed by coordination of carbon - carbon double bonds in a rate determining step (Equation 3.9) before the final rapid elimination of products and regeneration of the ruthenium monophosphine complex.

$$RuHCl(CO)(PCy_3) + H_2 \overset{K_2}{\rightleftharpoons} Ru(H_2)HCl(CO)(PCy_3) \quad (3.8)$$

$$Ru(H_2)HCl(CO)(PCy_3) + C=C \xrightarrow{k_{rds}} Ru(H_2)HCl(CO)(C=C)(PCy_3) \quad (3.9)$$

According to the proposed mechanism, the rate law of CPIP hydrogenation is given as follows:

$$-\frac{d[C=C]}{dt} = k_{rds}[Ru(H_2)HCl(CO)(PCy_3)][C=C] \quad (3.10)$$

The total concentration of ruthenium in the reactor is the amount of the styryl complex. If the formation of the active hydride from the styryl is rapid, the concentration of the styryl complex in solution will be negligible. Thus, the total Ru concentration in the system may be defined as in Equation 3.11.

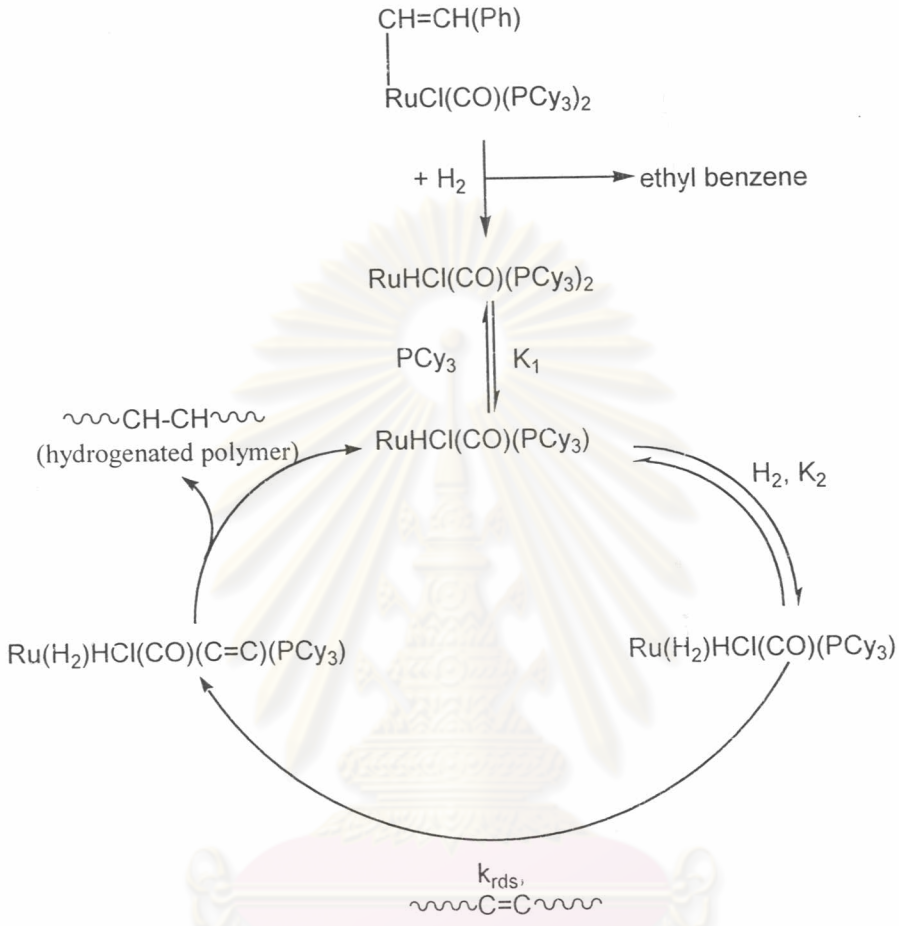

Figure 3.12: Proposed mechanism for hydrogenation of CPIP catalyzed by Ru(CH=CH(Ph))Cl(CO)(PCy_3)$_2$

$$[Ru]_T = [RuHCl(CO)(PCy_3)_2] + [RuHCl(CO)(PCy_3)] + [Ru(H_2)HCl(CO)(PCy_3)] \quad (3.11)$$

Assuming the equilibrium relations defined in Figure 3.12, the concentration of Ru $(H_2)HCl(CO)(C{=}C)(PCy_3)$ may be substituted into Equation 3.10 to provide the functional relationship between the observed pseudo first order reaction constant k' and the process factor studied (Equation 3.12).

$$k' = \frac{k_{rds}K_1K_2K_HP_{H_2}[Ru]_T}{K_1 + K_1K_2K_HP_{H_2} + [PCy_3]} \quad (3.12)$$

where K_H is the Henry's Law constant for hydrogen in chlorobenzene at 160°C.

The term $K_1K_2K_HP_{H2}$ in the denominator of Equation 3.12 is negligible due to the observed rigorous first order dependence on the hydrogen pressure over the range of study. Hence, the model reduces to the following form:

$$k' = \frac{k_4[Ru]_TP_{H_2}}{K_1 + [PCy_3]} \quad (3.13)$$

where the rate constant k_4 is a lumped constant containing the limiting reaction rate; k_{rds}, equilibrium constant K_1 and K_2, the Henry's Law constant for the solubility of hydrogen in chlorobenzene at 160°C; K_H.

In order to test the validity of the model given by Equation 3.13 with the observed kinetic data, the non-linear least square method for parameter estimation was employed. Regression estimates for the parameters are provided in Table 3.8 along with their associated error estimates. The results of an analysis of variance (ANOVA) summarized in Table 3.9 shows the significance of the model. The residue plot as illustrated in Figure 3.13 shows fairly random scattering of errors thus confirms that none of systematic error present. Figures 3.5b, 3.6b, and 3.8 show the observed experimental data along with the model predictions. Actual model predictions of olefin conversion profile relative to the data from gas uptake are plotted in Figures 3.14 and 3.15.

Table 3.8: Model Parameter Estimates

	Asymptotic 95 %			
	Asymptotic		Confidence Interval	
Parameter	Estimate	Std. Error	Lower	Upper
k_4, $(mM)^{-1}s^{-1}bar^{-1}$	6.89E-03	1.67E-03	3.37E-03	1.04E-02
K_1, $(mM)^{-1}bar^{-1}$	8.93E-02	2.24E-02	4.21E-02	1.37E-01

Table 3.9: Model Analysis of Variance Results

Source	DF	Sum of Squares	Mean Square
Regression	2	3.423	1.711
Residual	17	0.077	4.529E-03
Uncorrected Total	19	3.500	
(Corrected Total)	18	1.198	

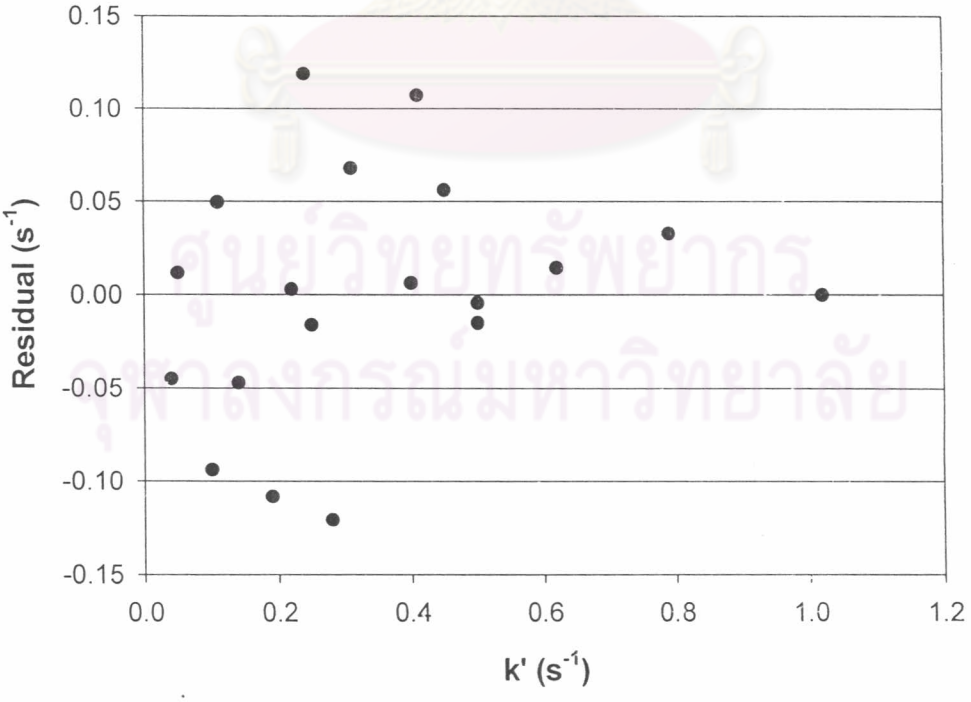

Figure 3.13: Residual plot from non-linear regression

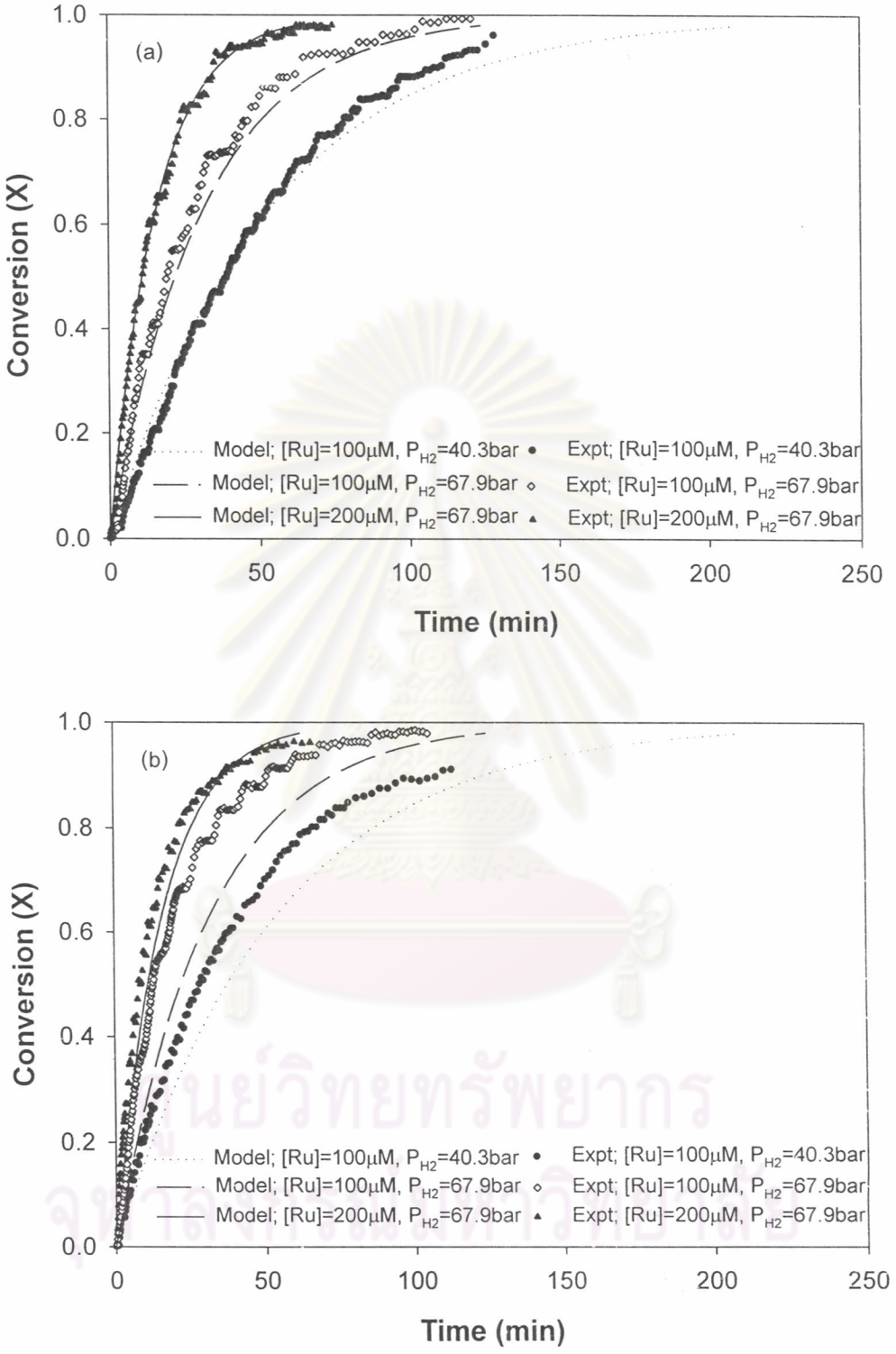

Figure 3.14: Comparison of the conversion profiles of experiment with model prediction for 2^3 factorial design experiments.
(a) Conversion profile at [C=C] = 130 mM; T = 160°C.
(b) Conversion profile at [C=C] = 520 mM; T = 160°C.

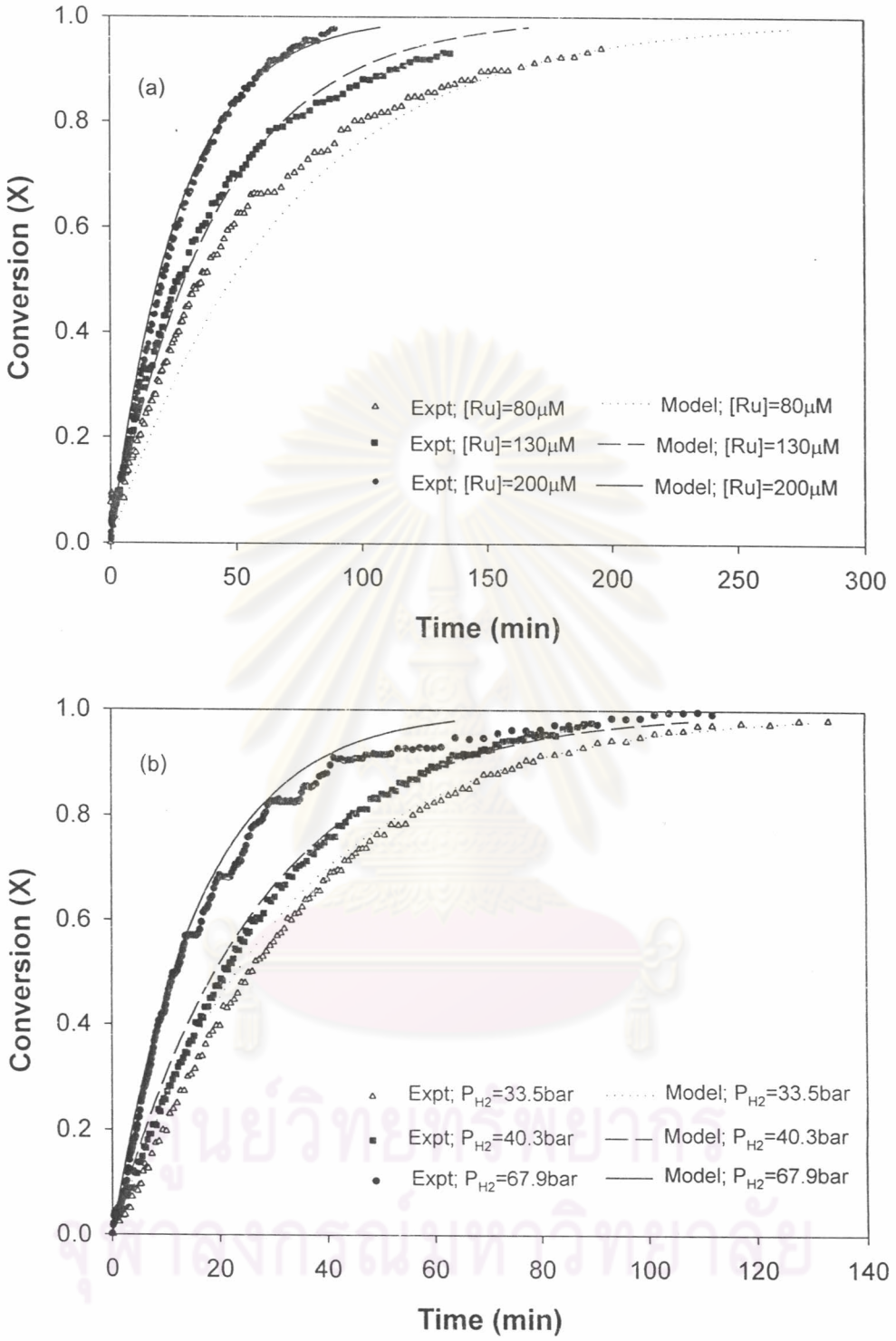

Figure 3.15: Comparison of the conversion profiles of experiment with model prediction for univariate kinetic experiments.
(a) Conversion profile at various with Ru concentration,
[C=C] = 260 mM; P_{H2} = 40.3 bar; T = 160°C.
(b) Conversion profile at various hydrogen pressure,
[C=C] = 260 mM; [Ru] = 200 μM; T = 160°C.